drift in conductivity for experiments where maximum temperature was maintained for 30 min. Given the demonstrably slow re-equilibration of magnesiowüstite with changing f_{O_2} (*15*), this evidence suggests that once the free oxygen was consumed by the pressure medium, $[Fe^{3+}]$ remained constant. We measured $[Fe^{3+}]$ in samples equilibrated under more reducing conditions using the change in unit cell parameter resulting from the incorporation of vacancies. A calibration curve of $[Fe^{3+}]$ against cell parameter was produced for large samples with the same total iron content equilibrated under gas mixtures using Mössbauer spectroscopy and XRD. The close agreement between predicted and measured $[Fe^{3+}]$ in samples equilibrated at given f_{O_2} demonstrated that the recoil-free fraction is equal in ferric and ferrous sites.

4. A. G. Duba and B. J. Wanamaker, *Geophys. Res. Lett.* **21**, 1643 (1994).
5. X. Li and R. Jeanloz, *J. Geophys. Res.* **95**, 21609 (1990).
6. H. K. Mao, *Carnegie Inst. Washington Yearb.* **72**, 554 (1973).
7. K. W. Hansen and I. B. Cutler, *J. Am. Ceram. Soc.* **49**, 100 (1966).
8. H. K. Mao, in *The Physics and Chemistry of Minerals and Rocks*, R. G. J. Strens, Ed. (Wiley, New York, 1976), pp. 573–582.
9. D. M. Sherman, *J. Geophys. Res.* **96**, 14299 (1991).
10. L. Volcado, A. Wall, S. C. Parker, G. D. Price, *Phys. Earth Planet. Inter.* **88**, 193 (1995).
11. Y. Xu and W. Y. Ching, *Phys. Rev. B* **43**, 4461 (1991).
12. Electronic charge carriers in ionic crystals cause significant strain on the lattice around the excess charge. This combination of the carrier and its associated strain field is the polaron. The mobility of the polaron depends on the mean drift between formation and trapping and the ease of accelerating the carrier in an electric field. Small polarons are bound to lattice sites and can only move by jumps between nearest or next-nearest neighbors, whereas large polarons are free to move in the conductance or valence band of the crystal and consequently have far higher mobilities.
13. H. L. Tuller, in *Point Defects in Minerals*, R. N. Shock, Ed. (American Geophysical Union, Washington, DC, 1985), pp. 47–68.
14. T. Goto, T. J. Ahrens, G. R. Rossman, Y. Syono, *Phys. Earth Planet. Inter.* **22**, 277 (1980); D. M. Sherman, *Phys. Chem. Miner.* **12**, 161 (1985).
15. J. Roberts *et al.*, *Eos* **76**, S156 (1995).
16. T. Katsura and E. Ito, *Geophys. Res. Lett.* **23**, 2005 (1996).
17. T. Irifune, *Nature* **370**, 131 (1994).
18. F. Guyot, M. Madon, J. Peyronneau, J. P. Poirier, *Earth Planet. Sci. Lett.* **90**, 52 (1990); B. J. Wood and D. C. Rubie, *Science* **273**, 1522 (1996).
19. We wish to thank N. Cohen and the University of London Intercollegiate Research Service in Mössbauer Spectroscopy for their assistance in Mössbauer analysis of samples and H. O'Neill for useful discussion in an early stage of this project. This work was supported by the Natural Environment Research Council.

22 October 1996; accepted 22 January 1997

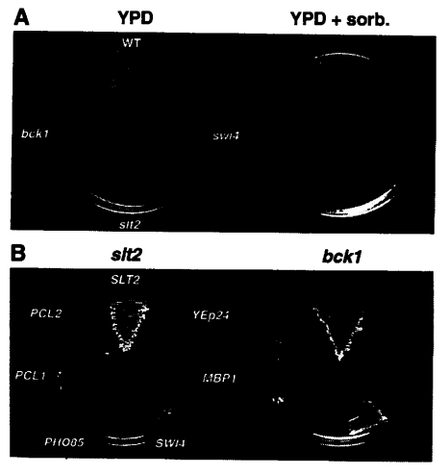

Fig. 1. Growth phenotypes of *SLT2* pathway and *swi4*Δ mutants, and suppression of the *slt2*Δ mutant by cell cycle regulatory components. (**A**) Growth of WT, *bck1*Δ, *slt2*Δ, and *swi4*Δ strains at 37°C on either rich YPD (yeast extract, peptone, dextrose) plates (left) or YPD plates containing 1 M sorbitol (right). (**B**) Assay for the suppression of the *slt2*Δ (left) and *bck1*Δ (right) growth defect at 37°C by either YEp24 vector alone or high–copy number plasmids containing either *SLT2*, *SWI4*, *PCL1*, *PCL2*, *PHO85*, or *MBP1* (*22*).

SBF Cell Cycle Regulator as a Target of the Yeast PKC–MAP Kinase Pathway

Kevin Madden, Yi-Jun Sheu, Kristin Baetz, Brenda Andrews, Michael Snyder*

Protein kinase C (PKC) signaling is highly conserved among eukaryotes and has been implicated in the regulation of cellular processes such as cell proliferation and growth. In the budding yeast, *PKC1* functions to activate the *SLT2(MPK1)* mitogen-activated protein (MAP) kinase cascade, which is required for the maintenance of cell integrity during asymmetric cell growth. Genetic studies, coimmunoprecipitation experiments, and analysis of protein phosphorylation in vivo and in vitro indicate that the SBF transcription factor (composed of Swi4p and Swi6p), an important regulator of gene expression at the G_1 to S phase cell cycle transition, is a target of the Slt2p(Mpk1p) MAP kinase. These studies provide evidence for a direct role of the *PKC1* pathway in the regulation of the yeast cell cycle and cell growth and indicate that conserved signaling pathways can act to control key regulators of cell division.

The coordination of polarized growth and cell proliferation is a critical process in many cell types. In yeast, the *PKC1* MAP kinase cascade functions to maintain the integrity of the cytoskeleton and cell wall (*1*, *2*) and is a candidate regulatory system for coupling cell growth and proliferation. The PKC pathway contains Pkc1p, which activates a MAP kinase cascade that consists of sequentially activated protein kinases: Bck1p(Slk1p), a MAP kinase extracellular signal–regulated kinase (MEK) kinase (MEKK), the redundant Mkk1 and Mkk2 MEKs, and Slt2p(Mpk1p), a MAP kinase (*3*). Genetic evidence has implicated this pathway in the regulation of cell cycle progression (*4–6*). In addition, the Slt2p MAP kinase is specifically activated during bud emergence and mating projection formation, periods of the cell cycle during which cell growth is highly polarized (*7*, *8*).

The SBF transcription factor also regulates both the yeast cell cycle and polarized growth (*9*). SBF is a heterodimeric complex composed of the Swi4p and Swi6p proteins (*10*). SBF regulates the transition from G_1 into S phase by activating the expression of the G_1 cyclin genes *CLN1*, *CLN2*, *PCL1*, and *PCL2* (*11–13*). Cln and Pcl proteins associate with the Cdc28 (*14*) and Pho85 (*13*) cyclin-dependent kinases, respectively, to promote entry into S phase; Cln-Cdc28p complexes also promote polarized growth (*15*). Thus, both SBF and PKC function to mediate cell cycle progression and polarized growth.

We used a genetic screen (*16*, *17*) to identify a mutation in the *SWI4* gene, *swi4-100*, that requires *SPA2* for growth (*18*). The Spa2 protein localizes to sites of polarized growth in yeast and is required for mating projection formation and proper bud site selection (*19*). Mutation of *SLT2* or *BCK1* is also lethal in the absence of *SPA2* (*16*). Moreover, other similarities are observed between *swi4*Δ and *SLT2* pathway mutants. Deletion of each kinase in the *SLT2* cascade results in temperature-sensitive growth, and at 37°C cells die by lysis; this temperature-sensitive growth defect is suppressed by the osmotic stabilizer 1 M sorbitol (*3*, *16*) (Fig. 1A). Haploid *swi4*Δ mutants are also temperature-sensitive for growth at 37°C in some backgrounds (*11*), and like *SLT2* pathway mutants, this temperature sensitivity is suppressed by the presence of 1 M sorbitol (Fig. 1A). Also, *swi4*Δ mutants exhibit a defect in projection formation upon exposure to mating pheromone, as do *SLT2* pathway mutants (*5*, *8*, *16*, *18*).

The phenotypic similarities between

K. Madden, Y.-J. Sheu, M. Snyder, Department of Biology, Yale University, Post Office Box 208103, New Haven, CT 06520–8103, USA.
K. Baetz and B. Andrews, Department of Molecular and Medical Genetics, University of Toronto, 1 King's College Circle, Toronto, Ontario M5S 1A8, Canada.
*To whom correspondence should be addressed.

slt2Δ and *swi4Δ* mutants indicate that *SLT2* and SBF may function in the same pathway. Because Swi4p and Swi6p are phosphoproteins in vivo (*20*) and the regulation of transcription factors through MAP kinase signaling has been shown in other systems (*21*), we investigated whether SBF might be activated by Slt2p (*22*). Plasmids containing either *SWI4*, *SWI6*, *MBP1*, *PHO85*, or G_1 cyclin genes were transformed into both *slt2Δ* and *bck1Δ* strains, and transformants were assayed for suppression of the 37°C temperature-sensitive growth defect. Overexpression of *SWI4* (*23*), *PCL1*, or *PCL2* suppressed the 37°C growth defect (Fig. 1B). Overexpression of *MBP1*, *PHO85* (Fig. 1B), *CLN1*, *CLN2*, *CLN3*, or *SWI6* failed to rescue the growth defect of *bck1Δ* or *slt2Δ* mutants at 37°C. High-copy *SLT2* plasmids were also transformed into *swi4Δ* mutants; these plasmids did not suppress the temperature-sensitive growth of *swi4Δ* strains at 37°C. Taken together, these observations support the hypothesis that SBF functions downstream of *SLT2*.

In addition to allowing *SLT2* pathway mutants to grow at 37°C, overexpression of *SWI4*, *PCL1*, or *PCL2* suppressed the cell lysis phenotype of these mutants both during vegetative growth and upon exposure to mating pheromone. After treatment with mating pheromone, wild-type cells arrest in late G_1 and undergo a prolonged period of polarized growth to form a mating projection; exposure of *slt2Δ* and other pathway mutants to mating pheromone (*24*) caused a fraction (37%) of cells to lyse, and few cells formed wild-type projections (Fig. 2A) (*5*, *8*). Overexpression of *SLT2*, *PCL1*, or *PCL2* or addition of 1 M sorbitol to the medium suppressed both the lysis and projection formation defects of *slt2Δ* cells (Fig. 2, B, C, E, and F). Overexpression of *SWI4* caused a decrease in cell lysis and a slight increase in the percentage of cells that formed wild-type projections (Fig. 2D). The *slt2Δ* strains overexpressing *SWI4* had an increased percentage of budded cells in the presence of mating pheromone (Fig. 2), probably because of the increased expression of the *CLN1* and *CLN2* cyclin genes mediated by Swi4p (*9*, *11*); Cln1p and Cln2p inhibit the pheromone response pathway (*25*). In summary, overexpression of *SWI4* and the *PCL* G_1 cyclin genes can suppress multiple phenotypes of *SLT2* MAP kinase pathway mutants, but overexpression of *SLT2* cannot rescue *swi4Δ* defects.

An examination of the various in vivo species of Swi6p further supported the hypothesis that SBF functions downstream of *SLT2* and suggested that the *SLT2* MAP kinase pathway may regulate the phosphorylation state of Swi6p (Fig. 3A). Immunoblot analysis with affinity-purified antibodies to Swi6p (anti-Swi6p) (*26*) revealed two major isoforms of Swi6p in lysates from log-phase cells (Fig. 3A). Phosphatase treatment (*27*) of Swi6p immunoprecipitates resulted in the loss of the slowly migrating species and an increase in the faster migrating isoform (Fig. 3A); the presence of the phosphatase inhibitor sodium molybdate prevented this conversion. Thus, the slowly migrating species is a phosphorylated form of Swi6p. A strain overexpressing *SLT2* accumulated the slowly migrating phosphorylated Swi6p isoform, whereas only the faster migrating Swi6p isoform was detected in strains lacking *SLT2* (Fig. 3A). Expression of a stable but inactive kinase allele, *slt2K54R* (*7*), in a *slt2Δ* strain did not increase accumulation of the slowly migrating isoform, indicating that the presence of phosphorylated Swi6p requires the kinase activity of Slt2p.

Swi6p phosphorylation correlates with the activity of Slt2p in vivo. Slt2p activity is stimulated by growth at increasing temperatures or by treatment of cells with mating pheromone (*7*, *8*, *28*). In cells grown at 30°C, the faster migrating form was the major Swi6p isoform detected, whereas incubation of cells at 39°C for 1 hour or exposure to mating pheromone resulted in the accumulation of phosphorylated Swi6p (Fig. 3A). The presence of intermediate species may indicate that several phosphorylation events occur. Cells exposed to a high concentration of pheromone for 2 hours and then washed and diluted into fresh medium for 15 min have low Slt2p activity (*7*) and also have an increase in the faster migrating isoform of Swi6p (Fig. 3A).

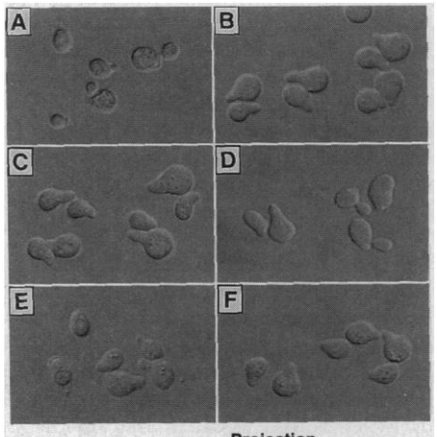

Plasmid	Lysed	Budded	Projection ≥0.33	Projection <0.33	Other	*n*
(A) YEp24	37	21	2	40	0	830
(B) SLT2	0	2	61	37	0	867
(C) YEp + sorb.	5	9	57	28	1	857
(D) SWI4	9	28	6	56	1	849
(E) PCL1	18	17	14	50	1	899
(F) PCL2	10	9	34	45	2	856

Fig. 2. Suppression of the lysis or projection formation defects (or both) of *slt2Δ* mutants exposed to mating pheromone by overexpressed *SWI4*, *PCL1*, and *PCL2* (*24*). (Top) Haploid *MATa slt2Δ* cells transformed with either YEp24 vector (**A**) or high copy plasmids containing *SLT2* (**B**), *SWI4* (**D**), *PCL1* (**E**), or *PCL2* (**F**) were treated with yeast α-factor. *slt2Δ* cells transformed with YEp24 were also grown in medium containing 1 M sorbitol (**C**) and exposed to pheromone. (Bottom) Quantitation of the percentage of cells ($n \geq 830$ cells) from strains described above that display lysis and projection formation defects (*24*).

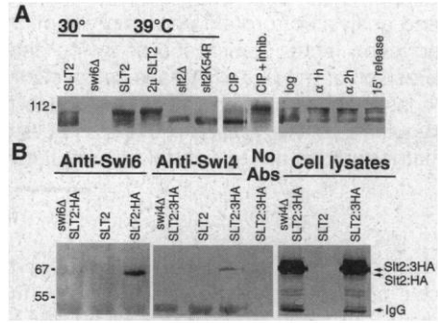

Fig. 3. In vivo evidence for Slt2p-dependent phosphorylation of Swi6p and coimmunoprecipitation of Slt2p and SBF. (**A**) Immunoblot analysis of Swi6p. Extracts were prepared from the following strains (*7*): Left seven lanes: wild-type strain PZY143 (SLT2); PZY181 (2μ SLT2) that overexpresses *SLT2*; YK193 (slt2K54R), a *slt2Δ* mutant that overexpresses a kinase-inactive allele of *SLT2*; YK175 (swi6Δ); and Y783 (slt2Δ). Strains were either grown at 30°C or shifted to 39°C for 1 hour before preparation of extracts (*28*). Right four lanes: Wild-type strain CMY826 was used for pheromone treatment (α 1h, α 2h) and α-factor block and release experiments (15′ release), as described (*7*). Approximately 5 μg of total yeast protein was loaded for each sample. CIP treatment experiments (*27*) and immunoblot analysis (*36*) were done as described. (**B**) Coimmunoprecipitation of Swi6p and Swi4p with Slt2p. (Left) Immunoblot analysis of Swi6p IPs from extracts of either a *swi6Δ* strain containing high-copy plasmid *SLT2:HA* (*7*) or from *SWI6* strains PZY143 (SLT2) and PZY181 (SLT2:HA) (*7*). (Middle) Immunoblot analysis of Swi4p IPs from extracts of *swi4Δ SLT2:3HA* cells, *slt2Δ* cells containing either high-copy *SLT2* or *SLT2:3HA* plasmids, or an experiment in which no antibody to Swi4p was added. *SLT2:3HA* contains three copies of sequence encoding the HA epitope at the COOH-terminal coding segment of *SLT2* in YEp352. (Right) Immunoblot analysis of total cellular protein (2 μg) from *swi4Δ SLT2:3HA* cells and *slt2Δ* cells containing either high-copy *SLT2* or *SLT2:3HA* plasmids; similar results were observed with *SLT2:HA* cell lysates. Cell extracts were prepared from strains incubated at 39°C for 1 hour. For the Swi6p and Swi4p IP experiments, 2 mg of total yeast protein and either affinity-purified rabbit anti-Swi6p (*26*) or anti-Swi4p (*37*) were used. After electrophoresis, proteins were blotted onto Immobilon-P (Millipore), probed with monoclonal antibody 12CA5 (BABCO), and primary antibodies were detected with alkaline phosphatase–conjugated goat anti-mouse IgG and the BCIP-NBT color substrate reaction (*35*).

Thus, for each of these different growth conditions, phosphorylation of Swi6p correlates with the level of Slt2p activity.

SBF was found to exist in a complex with Slt2p and therefore might be a direct target of Slt2p in vivo. Overexpression of *SLT2* tagged with either a single (*SLT2:HA*) (*7*) or three copies (*SLT2:3HA*) of the hemagglutinin (HA) epitope complemented the 37°C growth defect of *slt2Δ* cells. Immunoblot analysis with a monoclonal antibody to the HA epitope detected Slt2:HAp as a 64-kD protein and Slt2:3HAp as a 68-kD protein (Fig. 3B). We used affinity-purified antibodies to immunoprecipitate Swi6p or Swi4p from lysates of *slt2Δ* cells that overexpressed *SLT2*, *SLT2:HA*, or *SLT2:3HA*. Immunoblot analysis with an antibody to HA revealed that Slt2:HAp was present in Swi6p immunoprecipitates (IP) (Fig. 3B). A small amount of Slt2:3HAp (and Slt2:HAp) also coimmunoprecipitated with Swi4p (Fig. 3B). The majority of Slt2:HAp or Slt2:3HAp was detected in the supernatant of the immunoprecipitation, indicating that only a small fraction of the kinase is associated with either Swi6p or Swi4p, as might be expected for a kinase-substrate interaction. Association of Swi4p and Swi6p with Slt2:HAp was not detected in lysates from *swi4Δ* or *swi6Δ* strains or from strains expressing *SLT2* with no HA tag; furthermore, antibodies to the yeast Axl2 protein did not immunoprecipitate Slt2:HAp.

In vitro kinase assays indicated that Slt2p can directly phosphorylate Swi6p and Swi4p. Kinase assays with Slt2:3HAp (and Slt2:HAp) immunoprecipitated from yeast extracts exhibited phosphorylation of the immunoglobulin G (IgG) heavy chain, Slt2:3HAp itself, and a third phosphoprotein of ~100 kD (Fig. 4A). Immunoprecipitated Slt2:3HAp also phosphorylated myelin basic protein (*7*, *8*, *28*). Addition of Swi6p, purified from bacterial extracts (*26*), to the Slt2:HAp kinase reaction resulted in Swi6p phosphorylation (Fig. 4B); several phosphorylated isoforms were observed. A phosphoprotein of the expected size of Swi6p was not detected in kinase reactions that lack Swi6p or in kinase assays done on the Swi6p extracts alone (Fig. 4B).

Addition of partially purified insect cell extract containing Swi4p and Swi6p (*29*) to the Slt2:3HAp kinase assay resulted in the phosphorylation of a protein that migrated more slowly than Swi4p, yet appeared to be a phosphorylated form of Swi4p (Fig. 4A) (*29*); immunodepletion of Swi4p from the extracts before the kinase assay decreased the amount of this phosphoprotein (Fig. 4A). Thus, both Swi6p and Swi4p are substrates of Slt2:HAp in vitro.

To determine if Slt2p functions as a positive regulator of SBF activity, we performed RNA blot analysis (*26*) of four SBF-dependent genes, *CLN1*, *CLN2*, *PCL1*, and *PCL2*, with RNAs isolated from wild-type and *slt2Δ* strains (*30*). No differences in expression levels were detected for any of these genes in strains grown at either 25° or 30°C. However, when strains were incubated at 37°C for 3 hours, the amounts of *PCL1* and *PCL2* mRNAs in *slt2Δ* strains were one-half to two-thirds that of wild-type cells; this reduction is similar to the *SLT2*-dependent expression of several SBF-regulated genes involved in cell wall biosynthesis (*23*). No difference was detected in amounts of *CLN1* or *CLN2* mRNA. Thus, *SLT2* apparently functions to activate SBF; this activation results in the increased overall expression of a subset of SBF-dependent genes.

Although our data indicate that Slt2p activates SBF, the observation that *swi4* and *pkc1* as well as *swi4* and *slt2* are colethal (*18*, *23*) predicts that SBF and Slt2p may also have independent functions. Consistent with this interpretation, strains lacking SBF activity arrest predominantly in G_1 (*11*, *12*), whereas *slt2Δ* strains grown at 25°, 30°, or shifted to 37°C did not reveal an increase in the proportion of G_1 cells (*30*); this suggests that other mechanisms may contribute to the regulation of SBF target genes. Substrates of Slt2p besides SBF may also exist; one candidate is the potential transcription factor Rlm1p (*31*).

Our results indicate that the activation of Slt2p results in phosphorylation and activation of the SBF transcription factor, enabling SBF to promote the expression of the *PCL1* and *PCL2* G_1 cyclins and additional genes that regulate cell wall biosynthesis (*23*). The suppression of the *slt2Δ* temperature-sensitive growth defect by overexpressing *PCL1* or *PCL2* suggests a dual role for the Pcl-Pho85p complex in maintaining cell integrity and promoting cell cycle progression (*13*). In addition, the proper activation of Slt2p requires the Cdc28p kinase (*7*), indicating that the *PKC1* MAP kinase pathway is both activated by and an activator of cyclin-dependent kinase signaling; this regulation should result in a rapid amplification of G_1 kinase activity. The identification of SBF as a target of Slt2p offers insight into how PKC signaling regulates the G_1 kinase activity required for coordinating entry into S phase and polarized growth events. Because PKC (*32*) and MAP kinases (*21*) function to activate transcription factors that control cell proliferation in other organisms, this mode of PKC regulation may be a general mechanism.

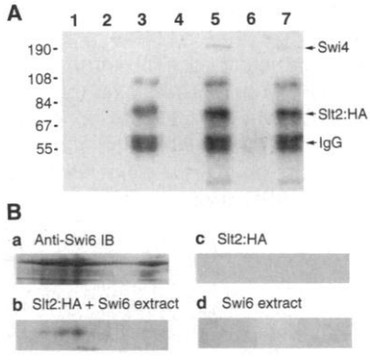

Fig. 4. In vitro phosphorylation of SBF by Slt2p (*29*). (**A**) Autoradiograph of gel blot of samples from in vitro phosphorylation reactions containing Swi4p. Kinase reactions were done without immune complexes (lane 1), with immune complexes isolated from yeast extracts containing Slt2:3HAp (lanes 3, 5, and 7), or with immunoprecipitates from extracts containing untagged Slt2p (lanes 4 and 6). Either a Swi4p or Swi6p preparation from insect cell extracts (*29*) (lanes 1, 5, and 6) or a preparation in which Swi4p was immunodepleted (lanes 2 and 7) was added to the reactions. For lanes 3 and 4, the reactions lacked the Swi4p or Swi6p extracts. (**B**) Autoradiograph and immunoblot analysis of blots from two-dimensional gels containing Swi6p phosphorylated in vitro by Slt2p (*38*). (a) Immunoblot analysis with affinity-purified anti-Swi6p of kinase reactions containing Slt2:HA IP and Swi6p purified from bacterial extracts (*26*, *36*). (b) Autoradiograph of the same blot that was probed with anti-Swi6p to generate (a). The left three Swi6p isoforms from (a) and (b) are superimposable. (c and d) Autoradiographs of kinase reactions containing either Slt2:HA IP immune complexes or Swi6p extract alone, respectively. Immunoprecipitations and kinase reactions are as described (*29*), except that 1.25 mg of total yeast protein from lysates of PZY181 cells that had been shifted to 39°C for 1 hour were used for kinase reactions. Swi6p-containing extracts (1.5 μg) (*26*) were added per kinase reaction.

REFERENCES AND NOTES

1. L. Torres *et al.*, *Mol. Microbiol.* **5**, 2845 (1991).
2. D. E. Levin and E. Bartlett-Heubusch, *J. Cell Biol.* **116**, 1221 (1992); G. Paravicini *et al.*, *Mol. Cell. Biol.* **12**, 4896 (1992); D. E. Levin and B. Errede, *Curr. Opin. Cell Biol.* **7**, 197 (1995).
3. K. Lee and D. Levin, *Mol. Cell. Biol.* **12**, 172 (1992); K. Irie *et al.*, *ibid.* **13**, 3076 (1993); K. S. Lee *et al.*, *ibid.*, p. 3067.
4. K. S. Lee, L. K. Hines, D. E. Levin, *ibid.* **13**, 5843 (1993).
5. C. Mazzoni, P. Zarzov, A. Rambourg, C. Mann, *J. Cell Biol.* **123**, 1821 (1993).
6. C. J. DiComo, H. Chang, K. T. Arndt, *Mol. Cell. Biol.* **15**, 1835 (1995); B. A. Morgan, N. Bouquin, G. F. Merrill, L. H. Johnston, *EMBO J.* **14**, 5679 (1995); N. J. Marini *et al.*, *ibid.* **15**, 3040 (1996).
7. P. Zarzoz, C. Mazzoni, C. Mann, *EMBO J.* **15**, 83 (1996).
8. B. Errede *et al.*, *Mol. Reprod. Dev.* **42**, 477 (1995).
9. L. Breeden, *Curr. Top. Microbiol. Immunol.* **208**, 95 (1996).
10. B. J. Andrews and I. Herskowitz, *Cell* **57**, 21 (1989); M. Primig, S. Sockanathan, H. Auer, K. Nasmyth, *Nature* **358**, 593 (1992); J. Sidorova and L. Breeden, *Mol. Cell. Biol.* **13**, 1069 (1993).
11. J. Ogas, B. J. Andrews, I. Herskowitz, *Cell* **66**, 1015 (1991).
12. K. Nasmyth and L. Dirick, *ibid.*, p. 995; M. J. Fernandez-Sarabia, A. Sutton, T. Zhong, K. T. Arndt, *Genes*

Dev. **6**, 2417 (1992); M. Tyers, G. Tokiwa, B. Futcher, *EMBO J.* **12**, 1955 (1993).
13. F. H. Espinoza, J. Ogas, I. Herskowitz, D. O. Morgan, *Science* **266**, 1388 (1994); V. Measday, L. Moore, J. Ogas, M. Tyers, B. Andrews, *ibid.*, p. 1391.
14. H. E. Richardson, C. Wittenberg, F. Cross, S. I. Reed, *Cell* **59**, 1127 (1989); F. R. Cross, *Mol. Cell. Biol.* **10**, 6482 (1990).
15. D. J. Lew and S. I. Reed, *J. Cell Biol.* **120**, 1305 (1993).
16. C. Costigan, S. Gehrung, M. Snyder, *Mol. Cell. Biol.* **12**, 1162 (1992); C. Costigan and M. Snyder, *ibid.* **14**, 2391 (1994).
17. E. G. Flescher, K. Madden, M. Snyder, *J. Cell Biol.* **122**, 373 (1993).
18. C. Costigan, Y.-J. Sheu, K. Madden, unpublished data.
19. M. Snyder, *J. Cell Biol.* **108**, 1419 (1989); S. Gehrung and M. Snyder, *ibid.* **111**, 1451 (1990).
20. A. Amon, M. Tyers, B. Futcher, K. Nasmyth, *Cell* **74**, 993 (1993); J. M. Sidorova, G. E. Mikesell, L. L. Breeden, *Mol. Biol. Cell* **6**, 1641 (1995).
21. R. Treisman, *Curr. Opin. Cell Biol.* **8**, 205 (1996); J. E. Slansky and P. J. Farnham, *Curr. Top. Microbiol. Immunol.* **208**, 1 (1996).
22. Congenic wild-type (WT) (Y762), *bck1Δ::TRP1* (Y782), *slt2Δ::LEU2* (Y783), and *swi4Δ::HIS3* (YK74) strains were prepared (*11*, *16*). High-copy plasmids containing the yeast 2μ origin of replication and either *SLT2* (*16*), *PCL1* (*11*), *PCL2* (pBA623; Hind III–Sal I fragment from a genomic library plasmid cloned into pRS426), *PHO85* (BK55; YEp24 genomic library plasmid), *SWI4* (B327; 8-kb Sph I fragment including *SWI4* subcloned into YEp352), or *MBP1* [BK72; polymerase chain reaction product including *MBP1* and flanking sequence (shown to be functional) cloned into YEp24] were transformed into *slt2Δ* and *bck1Δ* strains. These plasmids are expected to be present at ~20 copies per cell (*33*). Transformants were streaked on plates containing synthetic media lacking uracil (*34*) and incubated for 3 days at 37°C.
23. J. C. Igual, A. L. Johnson, L. H. Johnston, *EMBO J.* **15**, 5001 (1996).
24. *slt2Δ* cells containing either YEp24, or *SWI4*, *PCL1*, or *PCL2* high-copy plasmids (Fig. 1) were grown to late-log phase in 5-ml cultures of synthetic medium lacking uracil (with or without 1 M sorbitol); cells were diluted to an absorbance at 600 nm of 0.1 and grown for 3 hours in fresh synthetic complete medium. Cells were then centrifuged, resuspended, and incubated for 2 hours in 5 ml of rich medium with or without 1 M sorbitol. α-Factor (Sigma) was then added (5 μg/ml), and after 1 hour an equivalent dose of pheromone was added to the culture. The incubation was continued for 1 hour, and cells were fixed with 3.7% formaldehyde and washed three times with phosphate-buffered saline. Cells were observed by differential-interference microscopy, and the level of suppression of *slt2Δ* mutant phenotypes was quantified. Cells were either lysed, budded, or arrested in response to pheromone. Cells arrested in response to mating factor were divided into two classes on the basis of projection length: either ≥ or < one-third the diameter of the cell at the widest point. "Other" category includes cells with more than one projection or cells that have undergone polarized growth events that could not clearly be classified as buds or mating projections.
25. M. Peter, A. Gartner, J. Horecker, G. Ammerer, *Cell* **73**, 747 (1993); M. Tyers and B. Futcher, *Mol. Cell. Biol.* **13**, 5659 (1993).
26. Y. Ho, S. Mason, R. Kobayashi, M. Hoekstra, B. Andrews, *Proc. Natl. Acad. Sci. U.S.A.* **94**, 581 (1997).
27. Affinity-purified anti-Swi6 was used to immunoprecipitate Swi6p from 1 mg of total protein isolated from cells containing high-copy *SLT2:HA*; the cells had been incubated at 39°C for 1 hour. Immunoprecipitates were resuspended in 45 μl of NEB (New England Biolabs) Buffer 3 with 1% SDS. After 5 min of incubation at 37°C, the supernatant was removed and diluted to 0.1% SDS in NEB Buffer 3 with either 30 U of calf intestinal alkaline phosphatase (CIP) or 30 U of CIP together with 4 mM sodium molybdate (CIP + inhib.). Phosphatase reactions were incubated for 30 min at 37°C, and then Swi6p was reimmunoprecipitated from the phosphatase reaction.
28. Y. Kamada, U. S. Jung, J. Piotrowski, D. E. Levin, *Genes Dev.* **9**, 1559 (1995).
29. Recombinant baculoviruses containing *SWI4* and *SWI6* were isolated from SF9 insect cells and coinfected into Hi5 cells, as recommended (Invitrogen). Two days after infection, cells were harvested, washed, and lysed in buffer D [50 mM tris-HCl (pH 8.0), 20% glycerol, 50 mM NaCl, 0.5 mM EDTA, 10 mM β-mercaptoethanol], yielding ~ 2.5 mg of total protein per milliliter. To separate SBF from insect cell kinase activity, we precipitated Swi4p and Swi6p by addition of ammonium sulfate to a final concentration of 20%. The sedimented protein was resuspended in buffer D and loaded onto a heparin-agarose column for further purification (Affigel Heparin, Bio-Rad). Swi4p and Swi6p were eluted in 300 to 500 mM (buffer D plus increasing NaCl) washes and concentrated to 0.1 mg/ml. Five microliters of partially purified protein was used per kinase reaction. Swi4p was immunodepleted by addition of 2 μl of antibodies (~25 mg/ml) to Swi4p to 10 μl of the protein preparation for 5 hours at 4°C followed by addition of 5 μl of protein A–Sepharose (Pierce) to this mixture. After a 2-hour incubation the supernatant was removed. Slt2:3HAp IP and kinase reactions were similar to those described (*28*), except that for each kinase reaction 250 μg of total yeast protein was used for the Slt2:3HAp IP. In addition, the kinase reaction was incubated 15 min before the addition of [γ-^{32}P]ATP, and the reaction was allowed to proceed for 50 min. Half of each reaction was separated in a 10% polyacrylamide gel and blotted; the filter was used for autoradiography.
30. K. Baetz, Y. Ho, K. Madden, unpublished data.
31. Y. Watanabe, K. Irie, K. Matsumoto, *Mol. Cell. Biol.* **15**, 5740 (1995).
32. E. Rosengurt, A. Rodriguez-Pena, M. Coombs, J. Sinnet-Smith, *Proc. Natl. Acad. Sci. U.S.A.* **81**, 5748 (1984); K. Kaibuchi, Y. Takai, Y. Nishizuka, *J. Biol. Chem.* **260**, 1366 (1985); D. A. Persons, W. O. Wilkinson, R. M. Bell, O. J. Finn, *Cell* **52**, 447 (1988); H. Michak *et al.*, *J. Biol. Chem.* **268**, 110 (1993).
33. G. D. Clark-Walker and G. L. G. Miklos, *Eur. J. Biochem.* **41**, 359 (1974).
34. F. Sherman, G. Fink, J. Hicks, *Cold Spring Harbor Laboratories—Methods in Yeast Genetics* (Cold Spring Harbor Laboratory, Cold Spring Harbor, NY, 1986).
35. E. Harlow and D. Lane, *Antibodies: A Laboratory Manual* (Cold Spring Harbor Laboratory Press, Cold Spring Harbor, NY, 1988).
36. Proteins were separated by SDS–polyacrylamide gel electrophoresis (PAGE; 10% gel), blotted onto Immobilon-P (Millipore), probed with affinity-purified anti-Swi6p, and primary antibodies were detected with alkaline phosphatase–conjugated goat anti-rabbit IgG and the bromochloroindolyl phosphate–nitro blue tetrazolium (BCIP-NBT) color substrate reaction (*35*).
37. B. J. Andrews and I. Herskowitz, *Nature* **342**, 830 (1989).
38. Samples for two-dimensional electrophoresis were suspended in SDS sample buffer, then treated so that the first-dimension sample buffer contained 9.5 M urea, 2.0% Triton X-100, 5% β-mercaptoethanol, and 1.6% Bio-Lyte 5/7 and 0.4% Bio-Lyte 3/10 ampholytes (Bio-Rad). First-dimension isoelectric focusing and second-dimension SDS-PAGE (10% gel) were performed as recommended (Mini-PROTEAN II, Bio-Rad). The SDS-PAGE gel was blotted (*36*) and exposed for autoradiography (*29*).
39. We thank C. Mann for strains and plasmids, Y. Ho for providing antibodies and extracts, and Y. Barral, C. Costigan, and C. Crews for critical comments on the manuscript. Supported by grants from the National Institutes of Health (GM36494) (M.S.), the Medical Research Council of Canada (B.A.), a Howard Hughes Medical Institute predoctoral fellowship (K.M.), and a Connaught predoctoral scholarship (K.B.).

4 November 1996; accepted 27 January 1997

Constitutive Transcriptional Activation by a β-Catenin–Tcf Complex in APC$^{-/-}$ Colon Carcinoma

Vladimir Korinek,* Nick Barker,* Patrice J. Morin, Dick van Wichen, Roel de Weger, Kenneth W. Kinzler, Bert Vogelstein, Hans Clevers†

The adenomatous polyposis coli (APC) tumor suppressor protein binds to β-catenin, a protein recently shown to interact with Tcf and Lef transcription factors. The gene encoding hTcf-4, a Tcf family member that is expressed in colonic epithelium, was cloned and characterized. hTcf-4 transactivates transcription only when associated with β-catenin. Nuclei of APC$^{-/-}$ colon carcinoma cells were found to contain a stable β-catenin–hTcf-4 complex that was constitutively active, as measured by transcription of a *Tcf* reporter gene. Reintroduction of APC removed β-catenin from hTcf-4 and abrogated the transcriptional transactivation. Constitutive transcription of *Tcf* target genes, caused by loss of APC function, may be a crucial event in the early transformation of colonic epithelium.

The product of the *APC* tumor suppressor gene has been observed to interact with β-catenin and has thus been proposed to regulate cellular signaling events (*1*). β-Catenin, originally identified on the basis of its association with cadherin adhesion molecules, is now widely recognized as an essential element of the Wingless-Wnt signaling cascade (*2*). In the absence of Wnt signals, APC simultaneously interacts with the serine kinase glycogen synthase kinase (GSK)–3β and with β-catenin. Phosphorylation of APC by GSK-3β regulates the interaction of APC with β-catenin, which in turn may regulate the signaling function of β-catenin (*3*). Wnt signaling appears to